Published in final edited form as:
Curr Opin Colloid Interface Sci. 2012 December ; 17(6): 350–359. doi:10.1016/j.cocis.2012.09.004.

Advances in cryogenic transmission electron microscopy for the characterization of dynamic self-assembling nanostructures

Christina J. Newcomb[1], **Tyson J. Moyer**[1], **Sungsoo S. Lee**[1], and **Samuel I. Stupp**[1,2,3,4,*]

[1]Department of Materials Science and Engineering Northwestern University, Evanston, IL, USA

[2]The Institute for BioNanotechnology in Medicine, Northwestern University, Chicago, IL, USA

[3]Department of Chemistry, Northwestern University, Evanston, IL, USA

[4]Department of Medicine, Northwestern University, Chicago, IL, USA

Abstract

Elucidating the structural information of nanoscale materials in their solvent-exposed state is crucial, as a result, cryogenic transmission electron microscopy (cryo-TEM) has become an increasingly popular technique in the materials science, chemistry, and biology communities. Cryo-TEM provides a method to directly visualize the specimen structure in a solution-state through a thin film of vitrified solvent. This technique complements X-ray, neutron, and light scattering methods that probe the statistical average of all species present; furthermore, cryo-TEM can be used to observe changes in structure over time. In the area of self-assembly, this tool has been particularly powerful for the characterization of natural and synthetic small molecule assemblies, as well as hybrid organic–inorganic composites. In this review, we discuss recent advances in cryogenic TEM in the context of self-assembling systems with emphasis on characterization of transitions observed in response to external stimuli.

Keywords

self-assembly; cryogenic transmission electron microscopy; amyloid fibril assembly; block copolymer assembly; hybrid materials; peptide amphiphile

1. Introduction

Molecular self-assembly is a promising area of interdisciplinary science, covering a broad range of topics, from rational design of synthetic small molecules and polymers to the folding and aggregation of proteins and nucleic acids. Microscopy is an essential tool for characterization of these self-assembling systems because in enables direct visualization of their nanometer-sized features. Among the microscopy techniques that are commonly used, cryogenic transmission electron microscopy (cryo-TEM) is uniquely suited to provide structural and dynamic information of assemblies. The sample is vitrified in solution allowing direct visualization of the structure with variation in concentration, pH, osmolarity,

*Corresponding Author: Prof. Samuel I. Stupp, Northwestern University, Institute for BioNanotechnology in Medicine, 303 E Superior 11-123 Chicago, IL 60611, USA. s-stupp@northwestern.edu.

or temperature. Self-assembled structures including multicomponent micelles [1, 2], toroids [3], vesicles [4–6], helices [7, 8], twisted ribbons, and fibers [9] have been explored extensively using cryo-TEM. With recent advances in computing and sample preparation, three-dimensional rendering using single particle reconstruction of viruses and proteins has become possible, complementing X-ray crystallography data. Cryo-TEM has also proven invaluable for characterization of intermediate protein assemblies or dynamic processes that would be difficult to study using diffraction of protein crystals [10]. In addition, the development of supramolecular "smart" materials that respond to external stimuli often result in morphology changes or dynamic events that occur within a solvent, necessitating cryo-TEM [11–13]. Here we review a subset of organic self-assembling systems and the application of cryo-TEM to study morphology, kinetics, and dynamics of these structures *in situ*. Furthermore, we briefly discuss the instrumentation and advances for improving the technique as well as complementary cryogenic techniques that may be used to characterize larger macroscale materials on the nanoscale.

2. Sample Preparation and Instrumentation

Unlike other techniques that probe the nanoscale dimensions of organic assemblies such as atomic force microscopy (AFM) or conventional TEM, cryo-TEM has minimal sample requirements and directly visualizes the sample through a film of vitrified solvent, reducing confounding factors during imaging. For example, AFM requires imaging on a flat substrate that can carry a net surface charge, possibly influencing the observed nanostructures. Additionally, measurements involve direct interaction between the cantilever and the sample potentially distorting the sample. Conventional TEM primarily relies on the introduction of foreign components such as heavy metal salts for increased contrast, and more importantly, the sample is dried. When the solvent is removed, the hydration shell of the organic material is lost and information of the hydrated, native structure of the assembly can be compromised. Furthermore, if changes in the system are monitored, these techniques require some form of chemical fixation, which can introduce confounding effects and may not maintain the native state of the sample. In contrast, cryo-TEM employs thermal fixation, which reduces molecular motion by vitrifying the sample in a thin layer of solvent, making it a powerful tool for visualizing hydrated, self-assembled structures.

Sample preparation for cryo-TEM requires adequate fixation and preservation of the nanostructure. Thermal fixation is achieved by rapidly plunge freezing the specimen into a cryogen to achieve a vitreous film with minimal solvent crystallization. During the process, the humidity is controlled in order to prevent the loss of volatiles (such as water vapor), which could introduce drying artifacts in the sample. To form an electron transparent film suitable for imaging with a final thickness less than approximately 300 nm, the sample is blotted with filter paper to remove excess solvent prior to plunging (Figure 1). Instruments for automated plunge freezing of specimens are commercially available, such as the FEI Vitrobot and the Leica EM GP. An ideal cryogen should have a high thermal conductivity to allow for rapid vitrification during plunging and a high heat capacity in order to minimize the Leidenfrost effect, whereby rapid boiling of the cryogen forms an insulating gas film surrounds the specimen, reducing the rate of cooling and resulting in poor vitrification. In practice, the cryogen of choice for aqueous solutions is typically liquid ethane, whereas liquid nitrogen is often used to vitrify organic solvents, due to the solubility of ethane in nonpolar solvents.

TEM has three mechanisms to produce contrast: atomic number dependent (Z) contrast (mass-thickness contrast), diffraction contrast, and phase contrast. For cryo-TEM, although Z- and diffraction contrast can contribute to the image, the most prevalent contrast mechanism for visualizing amorphous, organic-based nanostructures in a vitreous film is

phase contrast. Since the electron beam is set at a single accelerating voltage, the beam exhibits a narrow energy spread and is relatively "monochromatic." As the electron waves interact with the sample, there are phase changes that correlate with the inner electron potential of the sample, producing contrast between the sample and the surrounding vitrified solvent. To utilize this contrast mechanism practically, the instrument is under-focused, but this can emphasize features of a specific size, making imaging at multiple defocus planes important for assessing the entire sample. Furthermore, there is a tradeoff between contrast and resolution when using defocus-phase contrast; increased defocus augments the contrast at the expense of reduced spatial resolution. Furthermore, absolute measurements in cryo-TEM micrographs have some variability due to the effect of underfocus. To increase both image resolution and contrast, recent efforts in TEM instrumentation have been made toward the development of phase plates that could eliminate the need to use defocus as a source of image contrast [14]. Additional instrumentation is also available to increase resolution. For example, aberration correctors correct for imperfections in the lenses and are particularly useful for the characterization of periodic, low-Z materials [15].

Although cryo-TEM has a number of advantages over other methods for characterizing nanoscale features, there are a few limitations to consider. Radiation damage of the specimen is one of the primary limiting factors, and the rate of damage varies from sample to sample [16]. Imaging is typically performed under low-electron dose conditions; however, this limits the signal-to-noise ratio because excessively long exposures can result in drift or radiation damage. Imaging using a phase plate can significantly enhance the imaging capabilities of cryo-TEM, but phase plates are currently tedious to use and are still being further optimized for commercial production [14]. Cryo-TEM images are prone to a number of artifacts due to sample preparation and electron-sample interactions. During plunging, the solvent can freeze resulting in the formation of ice crystals that appear as dark streaks or hexagons (hexagonal ice). Also, electron dense spherical artifacts are often observed (frost particles). Irradiation of the vitreous film by the electron beam can also cause a spotty appearance due to crystallization of vitreous ice to cubic ice [16]. If the sample is not plunged in the proper humidified environment, the sample can dry and become distorted. For methodologies to interpret cryo-TEM images and the mostly commonly observed artifacts, we direct the reader to several thorough reviews [6, 17, 18]. Also, cryo-TEM is not the most appropriate method for quantification; other techniques such as X-ray or light scattering are important to corroborate the micrographs. Lastly, the sample thickness is limited to a few hundred nanometers, making cells and macroscale materials difficult to characterize *in situ*, although important information may be present at the nanoscale. Very recently, researchers have taken the challenge to directly plunge live cells to evaluate cytoskeletal elements and organelles [19, 20]. For samples that are too large for direct imaging, recent developments in cryogenic fixation and cryo-sectioning have enabled cryo-electron tomography and imaging on vitreous sections at liquid nitrogen temperatures. These methods have revealed new structures in biological samples that were not observed previously due to sample dehydration [21]. The development of these sample preparation techniques also holds promise for nanoscale characterization of meso- and macroscale materials.

3. Block Copolymer Assemblies

A rich array of synthetic, amphiphilic block copolymers has been used to generate a plethora of dynamic structures that undergo morphological changes in response to external stimuli. Amphiphilic block copolymers are comprised of distinct polymeric segments that typically have molecular weights of 1–100 kDa and are well known to self-assemble into nanostructures with a dense core and highly solvated corona. The alternating hydrophobic and hydrophilic blocks enable attributes such as solvent selectivity and distinct phase

separation behavior. For example, changes in the composition or solubility of the corona or core polymers can lead to transformations in morphology that can be utilized for medical applications such as controlled drug release [22]. Changes in temperature, pH, and solvent composition can influence polymer behavior and assembly in solution. Recently, multicompartment block terpolymers have been studied because of their interesting dynamic behavior in solution [1]. Transitions in the morphology of assembled polymeric structures over time can be studied by small-angle X-ray and neutron scattering, but these results can be difficult to interpret and can often overlook intermediate structures that exist between the original and final morphologies. Cryo-TEM provides an *in situ* snapshot of morphological evolution in response to a dynamic sample environment. Elucidation of block copolymer morphology using cryo-TEM has been reviewed previously [23]; here we focus on recent work involving systems that exhibit stimuli-response and their use of cryo-TEM to observe these transitions.

3.1. Stimuli-induced transitions of block copolymer assemblies

The development of pH responsive materials has recently become an area of interest for a variety of applications, including controlled drug delivery [24]. Amphiphilic block copolymers provide an attractive approach, as the differences in solubility of the polymer corona can cause either collapse or phase separation, ultimately altering the final morphology. To appropriately probe these solvent exposed assemblies, cryo-TEM is among the most useful methods for characterization. Schacher *et al.* investigated the effect of acidic pH of solutions containing the block terpolymer ABC, where A is hydrophobic, and B and C are pH dependent, oppositely-charged polyelectrolytes [2]. Cryo-TEM revealed a core-shell micelle with an extended corona that underwent a collapse at pH 4. Additionally, miktoarm star block terpolymers transformed from spherical micelles with a mixed corona to multicompartment micelles when the pH was increased [25]. The transition from multicompartment spherical micelles to mixed corona micelles has also been observed with ABC block terpolymers, where A has pH-dependent solubility, B is hydrophobic, and C is hydrophilic [26]. As the pH was raised, the pH-dependent block moved from the core to the corona, generating spherical micelles. In addition to pH-induced changes in the corona, changes in the size of specific block copolymer domains have produced changes in morphology. Cracking in vesicles was observed by cryo-TEM as a result of membrane swelling in the block terpolymer ABC, where A is hydrophilic, B is hydrophobic, and C has a pH dependent solubility [27]. Within the vesicle membrane, the pH-dependent block formed an intermediate layer between two hydrophobic layers. As the pH decreased, the pH-dependent layer became more hydrated and swelled, which resulted in an increase in vesicle size, and eventual cracking in the hydrophobic block domains.

A shift in pH is commonly used as a method for accelerated degradation of block copolymer domains leading to morphological transformations. The variation in structure that accompanies the change in composition during degradation of the block copolymers can be readily captured by cryo-TEM. For example, miktoarm star terpolymers made up of μ-[ABC], where A is hydrophobic, B is hydrophilic, and C is a hydrolytic block degraded due to hydrolysis at high pH [28]. Interestingly, unlike the ABC wormlike micelle assemblies at neutral pH, the degradation products of the block terpolymers, AB and C homopolymers, formed large, spherical assemblies with a single cylindrical protrusion over two weeks at pH 12 (Figure 2a – 2c). It should be noted that morphologies like the one in Figure 2a would be exceedingly difficult to characterize by other techniques, such as small angle neutron and X-ray scattering. Furthermore, hydrolytic degradation, which was accelerated at low pH, caused a change in morphology of AB, where A is hydrophilic and B is a hydrophobic from wormlike micelles to spherical micelles [29]. In an AB block copolymer, where B is hydrophobic with orthoester side chains, spherical micelles were observed to increase in

both diameter and polydispersity as a result of ester hydrolysis within the hydrophobic block [30]. The change in the size distribution of these spherical micelles, as revealed by cryo-TEM, was later shown to correlate with faster release of doxorubicin at lower pH for applications in drug delivery [31]. An AB block copolymer, where A and B are soluble in acidic and basic conditions, respectively, were shown to form vesicles with either an anionic or cationic corona, depending on the pH [32].

Cryo-TEM is also useful to characterize temperature-sensitive polymeric assemblies. Thermal annealing can drive the assembly of block copolymers towards a thermodynamic equilibrium, producing interesting changes in morphology. Additionally, blocks of thermosensitive units can be inserted into the polymer backbone to induce switches in morphology. Walther *et al.* investigated ABC thermoresponsive block terpolymers that switched from a mixed corona to a phase-segregated corona [33]. After several heating cycles, the phase-segregated corona micelles began to aggregate into superstructures to minimize the contact of the temperature-sensitive phase with the solution. In hydrophilic-lipophilic-fluorophilic ABC block terpolymers, crystalline fluorophilic domains in phase segregated micelles became more visible by cryo-TEM after processing steps that included thermal annealing [34]. Increased temperatures can also influence the size of block copolymer assemblies. For example, ABC hydrophilic-lipophilic-fluorophilic block copolymers that form monodisperse micelles increased in both size and polydispersity with more visible phase separation after heating (Figure 2d – 2e) [35]. The phase separation was a result of the formation of fluorophilic domains, which appear denser by cryo-TEM. In addition to heating, incubation at cooler temperatures has also been observed to alter morphologies. Cooling to 4°C and warming to room temperature changed both the size and morphology of AB hydrophilic-hydrophobic block copolymers [36]. These polymers transformed from cylindrical micelles to vesicles based on these cooling/warming cycles as seen by cryo-TEM.

3.2. Assemblies in Solvent Mixtures

Solvent composition plays a strong role in determining the assembly behavior of supramolecular assemblies. For example, in mixtures of organic and aqueous solvents, an increase aqueous content can promote the driving force for hydrophobic interactions, resulting in high kinetic barriers. Cryo-TEM is uniquely suited to visualize assemblies in aqueous or organic solvents or their mixtures. By mixing water and tetrahydrofuran (THF), Rybtchinski et al. demonstrated the pathway-dependent assembly of an amphiphilic perylene diimide -peptide complex [37]. Additionally, using a similar solvent mixture and a perylene diimide-PEG based molecule that assembled into twisted fibers, the Rybtchinkski group was able to show reversible supramolecular polymerization and depolymerization of the assemblies, which correlated with switching of photofunction [38].

In the case of block copolymers, solvents can be selective for specific polymer blocks, leading to morphological changes in assembly. Liu *et al.* investigated miktoarm star triblock copolymers, where the poly(ethylethylene) block switched from the core to the corona after the addition of THF [39]. As THF was added, the observed structure first switched from disks to wormlike and spherical micelles, and then to oblate ellipsoid micelles. Adding THF also caused an assembly change in an ABC block terpolymer from uniform cylindrical micelles to multicompartment cylinders that exhibited subdivided hydrophobic regions [40]. Controlling the shape of polymerosome stomatocytes, made up of a hydrophilic-hydrophobic AB block copolymer, was achieved through variation of THF concentration relative to dioxane, while the ratio of total organic solvent to water was held constant (Figure 2f – 2h) [41]. Solutions with higher THF content resulted in a smaller diameter of the opening of the stomatocyte because of the change in swelling and rate of phase change within the PS domain. These same polymerosome stomatocyte structures evolved over time

during dialysis in 50/25/25 mixtures of water/THF/dioxane [42]. Selection of organic solvent in mixtures with water had significant effects on the assembly of AB block coplymers, where A is hydrophobic and B is a carboxylic acid-functionalized silsesquioxane [43]. Vesicles were observed by cryo-TEM in dioxane, wormlike micelles in DMF, and spherical micelles in DMF/NaOH. These changes in structure were likely due to the change in ionization of the carboxylic acid in the different organic solvents. Cryo-TEM also has been used for near-instantaneous imaging of aqueous/organic mixtures. Vitrification of a solution of hydrophilic-hydrophobic AB block copolymers was performed almost immediately after spraying of water into THF with the block copolymer, which led to the formation of vesicles [44]. As the percentage of water increased relative to THF, the assemblies switched from wormlike micelles to spheres back to wormlike micelles. Finally, at 80/20 water/THF, the block copolymer formed vesicles. The dynamic assembly of spheres to wormlike micelles was also observed in cryo-TEM by varying the mixing times (7 ms to 70 ms) after water was sprayed into THF. Overall, cryo-TEM has enabled characterization of solvent, pH, and temperature-responsive behavior of block copolymers, revealing dynamic behavior and intermediate structures to explain assembly in solution. During dynamic processes, mixtures of different morphologies that are present after the addition of a stimulus can be difficult to characterize by light, neutron and x-ray scattering. Alternatively, the instantaneous capture by cryo-TEM allows for the characterization of both the orignal, mixed intermediate, and final block copolymer assemblies, which could help generate insight about structure changes. While techniques like DLS can lend support to conclusions about dynamic morphologies, ultimately the changes observed by cryo-TEM are essential for understanding dynamic assemblies. Furthermore, the use of cryo-TEM for visualizing the morphology of block copolymers has become a standard technique and will only continue to become mainstream for other self-assembling systems.

4. Peptide-based Molecules

Over the past decade, self-assembling peptide-based molecules have received great attention primarily because of their potential as novel biomaterials for regenerative medicine [45–47], as well as their significance in understanding the formation of insoluble amyloid fibrils that have been associated with several neurological disorders [48]. Because such supramolecular interactions occur in aqueous environments, cryo-TEM has been a valuable tool to visualize and study the self-assembly of a broad class of peptide-based materials including peptide amphiphile (PA) molecules [49–52], β-hairpin peptides [53, 54], coiled-coil peptides [55, 56], collagen mimetic peptides [57], polypeptides [57, 58], amphiphilic proteins [59], peptide macrocycles [60], and polymer-peptide conjugates [61]. Recently, this ability to capture and image the supramolecular nanostructures *in situ* has been employed to characterize the dynamic self-assembly of such molecules, highlighting the differences in nanostructures before and after various conditions or treatments.

4.1. Peptide Amphiphile Assemblies

Peptide amphiphiles (PAs) are a class of small molecules that contain a hydrophilic peptide segment covalently bonded to a short hydrophobic block. They are designed to self-assemble into defined nanostructures through the use of supramolecular interactions such as hydrophobic collapse and intermolecular hydrogen bonding. Early experiments with PAs investigated their ability to assemble into small protein-like aggregates [62] and flat two-dimensional morphologies including monolayers at the air-water interface [63, 64]. Our group has designed a broad class of PA molecules that self-assemble into high aspect ratio cylindrical nanofibers [49, 65–67] nanoribbons [9, 68], and nanobelts [69]. These filamentous assemblies of PA molecules can form self-supporting gels by salt screening of the charged residues [70–72] or they can interact with biopolymers to create hierarchical structures [73–75]. The supramolecular networks have been shown to promote various

bioactivities including spinal cord regeneration [76], bone and cartilage regeneration [77–79], ischemic tissue repair [51, 80, 81], cavernous nerve repair [82]. Furthermore, the supramolecular architecture of PAs affords a unique bioactive component to the material. For example, presentation of biological peptide epitopes in high aspect ratio nanofibers has demonstrated improved bioactivity as compared to their spherical micelle counterparts [83], and the filamentous nanostructures proved advantageous for applications in cancer therapy [84, 85].

Since PA molecules are designed to self-assemble in aqueous media, cryo-TEM has proven to be an invaluable technique to directly visualize their supramolecular behavior in their native, hydrated state. Bitton and coworkers observed that PAs self-assembled into helical ribbons and tubules, and transitioned to a spherical micelle morphology after mixing with co-surfactants [86]. Our group recently demonstrated that PA molecules bearing a hydrophobic, laminin-derived peptide (IKVAV) had a high propensity to self-assemble into bundles of nanofibers, and this interdigitation of nanostructures resulted in reduced surface area and decreased bioactivity [68]. Using cryo-TEM, it was found that incorporating more like-charge amino acids adjacent to the bioactive epitope increased the electrostatic repulsion between the fibers, suppressed the bundling nanofibers, and enhanced the bioactivity. We have also reported that cylindrical assemblies of PA nanofibers were capable of spontaneous crystallization in aqueous environments [87]. Hexagonal packing of the nanofibers was observed beyond a critical PA concentration, presumably due to increased electrostatic repulsion between the nanofibers. Overall, the ability to characterize PA assemblies in solution by cryo-TEM has been an important step toward elucidating the role of molecular design on the resulting nanostructure and function.

Cryo-TEM also enables the visualization of dynamic processes by imaging samples with variable concentration, time, pH, temperature, or mechanical force. For example, a time-dependent morphological transformation from a metastable state of short, twisted ribbons to more thermodynamically stable long, helical ribbons (Figure 3) have been observed. This change in morphology was attributed to changes in aromatic stacking of phenylalanine side chains [9]. The transition from twisted to helical ribbons was also observed by Danino et al. using a bolaamphiphile containing two lysine residues; given additional time, the helical ribbons further transition into nanotubes via a mechanism that was revealed using cryoTEM [88, 89]. In an effort to understand the supramolecular factors that control micelle shape, Shimada and colleagues characterized a PA molecule with an α-helix-forming peptide headgroup and observed a transformation from spherical to wormlike micelles over time [90]. By performing CD measurements, they identified an accelerated transition in the secondary structure of the molecule from α-helix to β-sheet with increased temperature; based on this thermal transition, the authors claimed that the β-sheet secondary structure was more thermodynamically favored and thus responsible for the sphere-to-wormlike transition over time. Shimada and colleagues also observed that fluid shear stress could also induce the supramolecular transformation of the same PA molecules from spherical to wormlike micelles irreversibly. They claimed that the resulting wormlike micelles are highly stable due to the β-sheet formation in the secondary structure of the molecules after shear flow [91]. Using cryo-TEM, bundles of nanofibers could be observed and the number of nanofibers increased within each bundle with increasing concentration.

The development of stimuli-responsive self-assembling materials enables the ability to respond to biological stimuli or local changes in the environment and ultimately provide a therapeutic agent or a dynamic platform for cell-material interactions. Webber and colleagues designed “switchable” PA nanofibers with a consensus substrate sequence specific to protein kinase A (PKA) [92]. Using cryo-TEM, the high-aspect-ratio nanofibers were shown to disassemble upon phosphorylation in the presence of PKA and re-assemble

upon treatment with alkaline phosphatase, an enzyme that cleaves the phosphate group (Figure 4a – 4d). Hartgerink and colleagues developed both a PA molecule and multidomain peptides to include a specific matrix metalloproteinase-2 (MMP-2) cleavage site to create a dynamic, extracellular mimetic that would allow cell-mediated proteolytic degradation of the network and subsequent remodeling with natural ECM [93, 94]. They characterized multidomain peptides containing an ABA motif where the A block provides solubility and the amphiphilic B block drives the self-assembly and displays the MMP-2 cleavage site. They observed that the enzyme-mediated digestion resulted in a morphological transformation from highly crosslinked nanofibers to small aggregated globular structures [93]. Cryo-TEM was also employed to investigate the cell-material interaction between dental stem cells and MMP-2 cleavable PA hydrogel scaffolds [94]. The recent trend to utilize cryo-TEM for characterization of dynamic self-assembling substrates as well as the interactions between cells and nanoscale structures may help to further elucidate the many functions they could have in biological systems as novel therapies.

4.2. Peptide-Polymer Conjugates

Dynamic morphologies of self-assembling amphiphilic molecules have also been achieved through the conjugation of peptides to synthetic polymers. Generally a hydrophilic polymer, such as PEO, or a hydrophobic polymer block has been attached to a peptide sequence designed to promote specific, tunable supramolecular interactions. Covalently linking short peptide sequences to block copolymers has produced interesting new morphologies that have characterized by cryo-TEM. For instance, reversible transitions of PEO-peptide-PEO block copolymers demonstrated the ability to assemble from spheres to larger aggregates and back to spheres with increasing temperature [61]. These temperature-dependent assemblies were only observed when a zwitterionic peptide sequence was chosen. In another study, two peptide sequences that non-covalently attach to form a coiled-coil structure were chosen to create a supramolecular triblock polymer [95]. One peptide was attached to a hydrophilic PEO block and the other was attached to PS. When characterized independently, both the peptide-PEO and PS-peptide formed spherical micelles, as visualized by cryo-TEM. When combined in solution, the supramolecular bonds created a PS-peptide/peptide-PEG conjugate that formed rodlike structures. Cryo-TEM was also used to visualize a change in nanostructure from spherical micelles to dis-assembled structures upon addition of the protease chemotrypsin [96]. This example used a beta-amyloid peptide sequence (KLVFF) conjugated to a PEO block. No assemblies were observed after enzymatic degradation of the peptide block by chemotrypsin. In each of these cases, cryo-TEM was used to show the dynamic behavior of peptide-polymer conjugates in solution.

4.3. Self-assembly of amyloids

Amyloids are abnormal fibrous deposits composed of peptides or proteins assembled with a dominant β-sheet conformation [97], and these insoluble aggregates are associated with several neurodegenerative diseases including Parkinson's disease (PD), Alzheimer's disease (AD), and Huntington's disease (HD) [48]. To find new treatments, it is of utmost importance to gain structural and supramolecular insight into the mechanism of amyloid fibril assembly; however, their dynamic nature has made it difficult to produce protein crystals for X-ray diffraction experiments. Alternatively, cryo-TEM and image-processing techniques have been valuable in providing three-dimensional structural information of several amyloids. For example, cryo-TEM has been used to characterize α-synuclein (α-syn) proteins, which are highly aggregated in patients with PD. Vilar *et al.* observed that a single α-syn filament, either straight or twisted, consisted of two protofilaments [98]. In addition, AD has been linked with the aggregation of amyloid β (Aβ) peptides, and Sachse *et al.* revealed by cryo-TEM that this amyloid fibril also consisted of two protofilaments,

and each protofilament was comprised of a supramolecular stack of two anti-parallel polypeptide chains [99].

The formation of Aβ fibrils has been found to require a secondary structural transition of Aβ peptides from α-helix to β-sheet. Pagel and colleagues investigated whether a change of pH could be a triggering mechanism for such a transformation [100]. By designing *de novo* a model peptide based on a α-helical coiled-coil motif with β-sheet favoring subunits, they observed by cryo-TEM that the model peptide self-assembled into globular aggregates at low pH, but transitioned into fibers and twisted ribbons at neutral pH. In addition to pH, the influence of salt on the self-assembly of Aβ peptides has also been investigated. Castelletto and coworkers observed that addition of NaCl to NH_2-βAβAKLVFF-COOH peptides, a key sequence involved in Aβ fibril formation, resulted in the conformational change of the fibrils from thin nanoribbons to the coexistence of wide, twisted fibers and nanotubes [101]. They proposed that salt enhanced the twisting of fibers by screening the charge both at the β-sheet surface and at the edges of the twisted tapes. In a subsequent study, they also investigated the influence of charge and aromatic stacking interactions on the supramolecular behavior of the amyloid peptide fragments [102]. When the N- and C-termini of the peptide were each modified to be neutral, they observed that the extent of nanofiber twisting decreased with increasing salt concentration, as evidenced by the change in supramolecular assembly from twisted to flat ribbon structures. They postulated that since salt can only screen the charged lysine residue, the resulting decrease of the dipole effect from the residue would disrupt the twisting of the nanoribbons.

Furthermore, there also has been an effort to disaggregate mature amyloid fibrils to prevent any further tissue damage. By investigating a number of surfactants, Han and colleagues found that cationic gemini surfactant micelles were able to effectively disassemble mature amyloid fibrils *in vitro*, as observed by structural evolution of fibrils into globular aggregates after only one hour incubation (Figure 4e – 4g) [103]. Overall, cryo-TEM has allowed the study of structural evolution of several amyloid fibrils in their dynamic state, and this technique will continue to play a critical role in moving forward to understand and find strategies to treat relevant neurodegenerative diseases.

5. Organic-Inorganic Hybrid Assemblies

Hybrid materials that contain both organic and inorganic components have gained recent interest due to their potential in a variety of applications including catalysis, photovoltaics, photonics, and biomaterials [104–106]. The addition of an organic component during crystal nucleation and growth is a common approach to control the morphology and polymorph of an inorganic phase [107, 108]. Alternatively, to achieve spatial control over the inorganic phase, the organic-based material can act as a template to pattern inorganic nanoparticles [105]. Traditionally, conventional TEM is used to study the morphology and crystalline properties of inorganic materials, but maintaining the hydrated state of the organic component is often crucial for understanding the behavior in solution. Cryo-TEM provides a means for directly imaging the inorganic phase as well as identifying crystallization phenomena that may be transient in solution. For example, Penn and coworkers investigated growth mechanisms of iron oxides in the absence of organic modifiers and identified oriented aggregates of mesocrystal intermediates during crystallization as precursors to large single crystals [109]. Also, researchers have recently have advanced the current understanding of crystal growth in biological systems using cryo-TEM due to its ability to identify transient phases of the inorganic component during mineralization [110, 111].

5.1. Inorganic-Organic Composites

A common approach to produce hybrid nanomaterials for chemical sensing or catalysis involves incorporation of metals or semiconducting components with an organic, supramolecular matrix designed to organize the inorganic phase or respond to external stimuli [11]. Cryo-TEM is a reliable technique to visualize the nucleation dynamics of inorganic phases and determine the morphology of organic-inorganic materials due to the increased atomic number and diffraction contrast mechanisms of the inorganic material. Müller *et al.* developed a number of organic-inorganic systems that rely on the block copolymer architecture to control the segregation of inorganic nanoparticles and confirmed their final morphologies using cryo-TEM [112]. For example, they investigated crosslinked miktoarm star polymers bearing three different arms: polystyrene, polybutadiene, and poly(2-vinylpyridine) (PVP). Metal salts that coordinate strongly with the PVP block were reduced to Au, Ag, or CdS nanoparticles, and depending on the solvent composition, various morphologies such as two parallel channels or one single channel of inorganic could be achieved [33]. They also developed water-soluble organo-silica hybrid nanowires composed of cylindrical polymer brushes that were condensed to form a silsesquioxane network in the core and resulted in a material that exhibited a liquid-crystalline phase at higher concentrations. Alternatively, Maayan *et al.* synthesized polyoxometalate nanoparticles by templating cesium dodecyl sulfate micelles and imaged the hybrids using cryo-TEM; they found that clustering improved catalytic aerobic oxidation of sulfides [113]. Another recent study employed the use of cryo-TEM to visualize a “yolk-shell” architecture encapsulating Au or SiO_2 nanoparticles within a thermoresponsive polymer shell. Using temperature as a variable, selective reduction of 4-nitrophenol and nitrobenzene was achieved, enabling selectivity of the metal nanoparticle catalysis [114]. Characterization of organic-inorganic systems using cryo-TEM is becoming more prevalent and is an important method for probing the structural information in solution, where many catalytic and chemical sensing reactions take place.

5.2. Biomineralization

Biominerals are organized, hierarchical organic-inorganic composites that are often produced under the direction of cellular processes involving organic molecules that act as a template for the mineral. Biominerals are of interest because they exhibit control over crystal polymorphism, orientation, and shape during synthesis and they possess superior mechanical properties as compared to their synthetic counterparts. The mechanism by which mineral nucleation and growth occurs at the organic interface is proposed to be through a transient (or in some cases, stabilized) amorphous mineral phase, making cryogenic techniques such as cryo-TEM are essential to prevent dissolution or crystallization of amorphous mineral precursors. Sommerdijk and coworkers used cryo-TEM and cryo-tomography to study a simplified model for mineralization involving calcium carbonate mineralization of a self-assembled monolayer. Monitoring their system over time, they directly identified the role of pre-nucleation clusters that precede the formation of amorphous mineral and are not predicted using classical nucleation theory [110]. Tester *et al.* investigated the stabilization of amorphous calcium carbonate confined within self-assembled liposomes of varying size using cryo-TEM [115]. Additionally, our lab has examined the role of peptide amphiphile nanostructure as a template for oriented hydroxyapatite mineralization [116]. Studies that directly involve protein templates have also been performed. *In vitro* mineralization of collagen bundles, the organic template in mammalian bone, was implemented to study the various stages of mineralization and understand how the mineral is incorporated into the organic component using cryo-TEM (Figure 5a – 5c), tomography (Figure 5d) and molecular modeling [117]. Similar techniques have also been performed on amelogenin, the protein template in enamel mineralization, to further elucidate mechanisms by which the protein assembles to accommodate the mineral

phase [118]. A recent study that used extensive electron microscopy directly imaged intracellular amorphous calcium phosphate-containing vesicles in developing bone [111]. In this work, cryogenic scanning electron microscopy of freeze-fractured bone, cryo-TEM of freeze dried or vitrified sections (Figure 4e – 4g), and electron diffraction were used in combination to identify calcium-phosphate-containing vesicles, which have been proposed to transport the mineral to the extracellular mineralization front.

Future and Outlook

With the increasing need for unambiguous characterization of self-assembling systems in their solvent-exposed state, direct imaging cryo-TEM is becoming the new standard for nanoscale characterization. Cryogenic sample preparation uniquely affords the study of stimuli-responsive structures and fragile materials that could otherwise dissolve or change in morphology using conventional TEM. Additionally, the emergence of cryogenic techniques for characterization of a variety of systems including self-assembling organic materials and even organic-inorganic interfaces in biomineralization implies that the use of cryo-TEM may be extended to many more research areas in the future. Also, with the recent development of techniques such as cryogenic imaging of vitreous sections, the scope of materials that can be applied to cryo-TEM is further extended, allowing elucidation of larger systems. One exciting direction includes the development in the technique allowing for studies of living cells and their native extracellular matrix. In the context of this review, this particular direction could enable research focused on the interactions of therapeutic synthetic structures for the fields of regenerative nanomedicine and targeted drug delivery with highly designed nanoscale objects.

Acknowledgments

The authors thank Liam Palmer for assistance with the manuscript. Research in the authors' laboratory described in this paper was supported by grants from the National Institutes of Health (Grant Numbers 2R01DE015920-06, 2R01EB003806-06A2, 1U54CA151880-01), the U.S. Department of Energy, Office of Basic Energy Sciences, Division of Materials Sciences and Engineering under Contract No. DE-FG02-00ER45810, DARPA Grant No. W911NF-09-1-0044, and the National Science Foundation Grant No. DMR-1006713. T.J.M. was supported by the National Science Foundation Graduate Research Fellowship and S.S.L. was supported by the Samsung Scholarship Foundation. The authors are also grateful for the use of experimental facilities at the Institute for BioNanotechnology in Medicine (IBNAM), the Biological Imaging Facility (BIF), the Integrated Molecular Structure Education and Research Center (IMSERC), the Northwestern University Atomic and Nanoscale Characterization Experimental Center (NUANCE, EPIC, NIFTI, Keck-II) and Keck Biophysics Facilities at Northwestern University.

References

1. Moughton AO, Hillmyer MA, Lodge TP. Multicompartment Block Polymer Micelles. Macromolecules. 2012; 45:2–19.
2. Schacher F, Walther A, Müller AHE. Dynamic multicompartment-core micelles in aqueous media. Langmuir. 2009; 25:10962–10969. [PubMed: 19537738]
3. Pochan DJ, Chen Z, Cui H, et al. Toroidal triblock copolymer assemblies. Science. 2004; 306:94–97. [PubMed: 15459386]
4. Voskuhl J, Fenske T, Stuart MCA, et al. Molecular Recognition of Vesicles: Host–Guest Interactions Combined with Specific Dimerization of Zwitterions. Chem Eur J. 2010; 16:8300–8306. [PubMed: 20593445]
5. Lim CW, Crespo-Biel O, Stuart MCA, et al. Intravesicular and intervesicular interaction by orthogonal multivalent host–guest and metal–ligand complexation. Proc Natl Acad Sci US A. 2007; 104:6986.
6. Kuntsche J, Horst JC, Bunjes H. Cryogenic transmission electron microscopy (cryo-TEM) for studying the morphology of colloidal drug delivery systems. Int J Pharm. 2011; 417:120–137. [PubMed: 21310225]

7. Lin Y, Wang A, Qiao Y, et al. Rationally designed helical nanofibers via multiple non-covalent interactions: fabrication and modulation. Soft Matter. 2010; 6:2031.
8. Xu Y, Bolisetty S, Drechsler M, et al. Manipulating cylindrical polyelectrolyte brushes on the nanoscale by counterions: collapse transition to helical structures. Soft Matter. 2009; 5:379.
9. Pashuck ET, Stupp SI. Direct Observation of Morphological Tranformation from Twisted Ribbons into Helical Ribbons. J Am Chem Soc. 2010; 132:8819–8821. [PubMed: 20552966]
10. Cyrklaff MM, Linaroudis AA, Krijnse-Locker JJ 7. Whole cell cryo-electron tomography reveals distinct disassembly intermediates of vaccinia virus. PLoS One. 2007; 2:1–10.
11. Fenske T, Korth HG, Mohr A, Schmuck C. Advances in Switchable Supramolecular Nanoassemblies. Chem Eur J. 2012; 18:738–755. [PubMed: 22170585]
12. Rybtchinski B. Adaptive Supramolecular Nanomaterials Based on Strong Noncovalent Iinteractions. ACS Nano. 2011
13. Nalluri SKM, Voskuhl J, Bultema JB, et al. Light-Responsive Capture and Release of DNA in a Ternary Supramolecular Complex. Angew Chem Int Ed. 2011; 50:9747–9751.
14. Danev, R.; Nagayama, K. Methods in Enzymology. Elsevier; 2010. Phase Plates for Transmission Electron Microscopy; p. 343-369.
15. Evans JE, Hetherington C, Kirkland A, et al. Low-dose aberration corrected cryo-electron microscopy of organic specimens. Ultramicroscopy. 2008; 108:1636–1644. [PubMed: 18703285]
16. Danino, D.; Talmon, Y. Direct-Imaging and Freeze-Fracture Cryo-Transmission Electron Microcopy of Molecular Gels. In: Weiss, R.; Terech, P., editors. Molecular gels. Materials with Self-Assembled Fibrillar Networks. Springer; 2005.
17. Friedrich H, Frederik PM, de With G, Sommerdijk NAJM. Imaging of self-assembled structures: interpretation of TEM and cryo-TEM images. Angew Chem Int Ed. 2010; 49:7850–7858.
18. Talmon, Y. Cryogenic Temperature Transmission Electron Microscopy in the Study of Surfactant Systems. In: Binks, BP., editor. Modern Characterization Methods of Surfactant Systems. Switzerland: Marcel Dekker, Inc; 1999. p. 147-177.
**19. Ben-Harush K, Maimon T, Patla I, et al. Visualizing cellular processes at the molecular level by cryo-electron tomography. J Cell Sci. 2010; 123:7–12. In this article, the authors demonstrate the ability to evaluate macromolecular complexes of a eukaryotic cell in situ without using conventional methods of sectioning. By using cryo-electron tomography, they were able to visualize the cytoskeleton, nuclear envelope, and even a nuclear pore by simply plunge freezing the cell. This type of visualization can open new perspectives on basic cell biology by being able to preserve the cell integrity without the use of chemical fixing, drying or cutting. [PubMed: 20016061]
20. Fernandez-Busnadiego R, Schrod N, Kochovski Z, et al. Insights into the molecular organization of the neuron by cryo-electron tomography. J Electron Microsc. 2011; 60:137–148.
21. Hurbain I, Sachse M. The future is cold: cryo-preparation methods for transmission electron microscopy of cells. Biol Cell. 2011; 103:405–420. [PubMed: 21812762]
22. Li M-H, Keller P. Stimuli-responsive polymer vesicles. Soft Matter. 2009; 5:927–937.
23. Zhong S, Pochan DJ. Cryogenic Transmission Electron Microscopy for Direct Observation of Polymer and Small-Molecule Materials and Structures in Solution. Polym Rev. 2010; 50:287–320.
24. Lee JS, Feijen J. Polymersomes for drug delivery: Design, formation and characterization. J Controlled Release. 2011 In Press. 10.1016/j.jconrel.2011.10.005
25. Liu C, Hillmyer MA, Lodge TP. Multicompartment micelles from pH-responsive miktoarm star block terpolymers. Langmuir. 2009; 25:13718–13725. [PubMed: 19438177]
26. Uchman M, Stepánek M, Procháka K, et al. Multicompartment Nanoparticles Formed by a Heparin-Mimicking Block Terpolymer in Aqueous Solutions. Macromolecules. 2009; 42:5605–5613.
27. Yu S, Azzam T, Rouiller I, Eisenberg A. “Breathing” vesicles. J Am Chem Soc. 2009; 131:10557–10566. [PubMed: 19722630]
*28. Saito N, Liu C, Lodge TP, Hillmyer MA. Multicompartment micelle morphology evolution in degradable miktoarm star terpolymers. ACS Nano. 2010; 4:1907–1912. Saito *et al.* present the morphology of muticompartment micelles in various conditions, including evolution to a new “rasberry-like vesicle” morphology over time, which is observed using cryogenic TEM. The new

morphologies that emerge are of great importance when keeping in mind applications where the material may experience a variety of environments over time. This type of characterization is particularly in self-assembling systems, which are dynamic and morphologies can be trapped in non-equilibrium morphologies for some time. Furthermore, particularly with block co-polymers, evaluation of phase separation over time is important. [PubMed: 20218703]

29. Geng Y, Discher D. Hydrolytic degradation of poly(ethylene oxide)-block-polycaprolactone worm micelles. J Am Chem Soc. 2005; 127:12780–12781. [PubMed: 16159254]
30. Tang R, Ji W, Wang C. Amphiphilic Block Copolymers Bearing Ortho Ester Side-Chains: pH-Dependent Hydrolysis and Self-Assembly in Water. Macromol Biosci. 2010; 10:192–201. [PubMed: 19904722]
31. Tang R, Ji W, Panus D, et al. Block copolymer micelles with acid-labile ortho ester side-chains: Synthesis, characterization, and enhanced drug delivery to human glioma cells. J Controlled Release. 2011; 151:18–27.
32. Du J, O'Reilly RK. pH-Responsive Vesicles from a Schizophrenic Diblock Copolymer. Macromol Chem Phys. 2010; 211:1530–1537.
33. Walther A, Barner-Kowollik C, Müller AHE. Mixed, multicompartment, or Janus micelles? A systematic study of thermoresponsive bis-hydrophilic block terpolymers. Langmuir. 2010; 26:12237–12246. [PubMed: 20465237]
34. Skrabania K, Laschewsky Av, Berlepsch H, Boettcher C. Synthesis and Micellar Self-Assembly of Ternary Hydrophilic-Lipophilic-Fluorophilic Block Copolymers with a Linear PEO Chain. Langmuir. 2009; 25:7594–7601. [PubMed: 19320429]
35. Marsat J-N, Heydenreich M, Kleinpeter E, et al. Self-Assembly into Multicompartment Micelles and Selective Solubilization by Hydrophilic-Lipophilic-Fluorophilic Block Copolymers. Macromolecules. 2011; 44:2092–2105.
36. Rank A, Hauschild S, Foerster S, Schubert R. Preparation of Monodisperse Block Copolymer Vesicles via a Thermotropic Cylinder-Vesicle Transition. Langmuir. 2009; 25:1337–1344. [PubMed: 19125559]

*37. Tidhar Y, Weissman H, Wolf SG, et al. Pathway-Dependent Self-Assembly of Perylene Diimide/Peptide Conjugates in Aqueous Medium. Chem Eur J. 2011; 17:6068–6075. Tidhar *et al.* describe various pathways of a self-assembling perylene diimide molecule and characterize the final morphologies by cryogenic TEM. Using this approach, they demonstrate that these assemblies can be trapped in kinetic minimia and can result in different morphologies. Furthermore, a mixture of organic solvent with water helps to control the degree of hydrogen bonding. These types of approaches can help the community to understand the complex energy landscape that many of these self-assembly molecules exhibit. [PubMed: 21542033]

38. Baram J, Shirman E, Ben-Shitrit N, et al. Control over self-assembly through reversible charging of the aromatic building blocks in photofunctional supramolecular fibers. J Am Chem Soc. 2008; 130:14966–14967. [PubMed: 18928256]
39. Liu C, Hillmyer MA, Lodge TP. Evolution of multicompartment micelles to mixed corona micelles using solvent mixtures. Langmuir. 2008; 24:12001–12009. [PubMed: 18788767]
40. Cui H, Chen Z, Zhong S, et al. Block Copolymer Assembly via Kinetic Control. Science. 2007; 317:647–650. [PubMed: 17673657]
41. Kim KT, Zhu J, Meeuwissen SA, et al. Polymersome Stomatocytes: Controlled Shape Transformation in Polymer Vesicles. J Am Chem Soc. 2010; 132:12522–12524. [PubMed: 20718470]
42. Meeuwissen SA, Kim KT, Chen Y, et al. Controlled Shape Transformation of Polymersome Stomatocytes. Angew Chem Int Ed. 2011; 50:7070–7073.
43. Yu X, Zhong S, Li X, et al. A Giant Surfactant of Polystyrene-(Carboxylic Acid-Functionalized Polyhedral Oligomeric Silsesquioxane) Amphiphile with Highly Stretched Polystyrene Tails in Micellar Assemblies. J Am Chem Soc. 2010; 132:16741–16744. [PubMed: 21049944]
44. Adams DJ, Kitchen C, Adams S, et al. On the mechanism of formation of vesicles from poly(ethylene oxide)-block-poly(caprolactone) copolymers. Soft Matter. 2009; 5:3086–3096.
45. Aida T, Meijer EW, Stupp SI. Functional supramolecular polymers. Science. 2012; 335:813–817. [PubMed: 22344437]

46. Matson JB, Zha RH, Stupp SI. Peptide self-assembly for crafting functional biological materials. Curr Opin Solid State Mater Sci. 2011; 15:225–235. [PubMed: 22125413]
47. Cui H, Webber MJ, Stupp SI. Self-assembly of peptide amphiphiles: from molecules to nanostructures to biomaterials. Biopolymers. 2010; 94:1–18. [PubMed: 20091874]
48. Ross CA, Poirier MA. Protein aggregation and neurodegenerative disease. Nat Med. 2004; 10 (Suppl):S10–S17. [PubMed: 15272267]
49. Hartgerink J, Beniash E, Stupp S. Self-assembly and mineralization of peptide-amphiphile nanofibers. Science. 2001; 294:1684–1688. [PubMed: 11721046]
50. Pashuck ET, Cui H, Stupp SI. Tuning supramolecular rigidity of peptide fibers through molecular structure. J Am Chem Soc. 2010; 132:6041–6046. [PubMed: 20377229]
51. Webber MJ, Tongers J, Newcomb CJ, et al. Supramolecular nanostructures that mimic VEGF as a strategy for ischemic tissue repair. Proc Natl Acad Sci US A. 2011; 108:13438–13443.
52. He C, Han Y, Fan Y, et al. Self-assembly of abeta-based Peptide amphiphiles with double hydrophobic chains. Langmuir. 2012; 28:3391–3396. [PubMed: 22272929]
53. Hule RA, Nagarkar RP, Altunbas A, et al. Correlations between structure, material properties and bioproperties in self-assembled beta-hairpin peptide hydrogels. Faraday Discuss. 2008; 139:251–264. [PubMed: 19048999]
54. Yucel T, Micklitsch CM, Schneider JP, Pochan DJ. Direct Observation of Early-Time Hydrogelation in beta-Hairpin Peptide Self-Assembly. Macromolecules. 2008; 41:5763–5772. [PubMed: 19169385]
55. Fletcher NL, Lockett CV, Dexter AF. A pH-responsive coiled-coil peptide hydrogel. Soft Matter. 2011; 7:10210–10218.
56. Dong H, Paramonov SE, Hartgerink JD. Self-assembly of alpha-helical coiled coil nanofibers. J Am Chem Soc. 2008; 130:13691–13695. [PubMed: 18803383]
57. O'Leary LER, Fallas JA, Bakota EL, et al. Multi-hierarchical self-assembly of a collagen mimetic peptide from triple helix to nanofibre and hydrogel. Nat Chem. 2011; 3:821–828. [PubMed: 21941256]
58. Pochan D, Pakstis L, Ozbas B, et al. SANS and Cryo-TEM study of self-assembled diblock copolypeptide hydrogels with rich nano- through microscale morphology. Macromolecules. 2002; 35:5358–5360.
59. Bachar M, Mandelbaum A, Portnaya I, et al. Development and characterization of a novel drug nanocarrier for oral delivery, based on self-assembled β-casein micelles. J Controlled Release. 2012 In Press. 10.1016/j.jconrel.2012.01.004
60. Carnall JMA, Waudby CA, Belenguer AM, et al. Mechanosensitive self-replication driven by self-organization. Science. 2010; 327:1502–1506. [PubMed: 20299594]
61. Choi BG, Cho S-H, Lee H, et al. Thermoreversible Radial Growth of Micellar Assembly for Hydrogel Formation Using Zwitterionic Oligopeptide Copolymer. Macromolecules. 2011; 44:2269–2275.
62. Forns P, Lauer-Fields JL, Gao S, Fields GB. Induction of protein-like molecular architecture by monoalkyl hydrocarbon chains. Biopolymers. 2000; 54:531–546. [PubMed: 10984405]
63. Berndt P, Fields GB, Tirrell M. Synthetic lipidation of peptides and amino acids: monolayer structure and properties. Journal Of The American Chemical Society. 1995; 117:9515–9522.
64. Bianco-Peled H, Dori Y, Schneider J, et al. Structural Study of Langmuir Monolayers Containing Lipidated Poly(ethylene glycol) and Peptides. Langmuir. 2001; 17:6931–6937.
65. Guler MO, Hsu L, Soukasene S, et al. Presentation of RGDS epitopes on self-assembled nanofibers of branched peptide amphiphiles. Biomacromolecules. 2006; 7:1855–1863. [PubMed: 16768407]
66. Pashuck ET, Cui H, Stupp SI. Tuning supramolecular rigidity of peptide fibers through molecular structure. J Am Chem Soc. 2010; 132:6041–6046. [PubMed: 20377229]
67. Huang Z, Newcomb CJ, Bringas P Jr, et al. Biological synthesis of tooth enamel instructed by an artificial matrix. Biomaterials. 2010; 31:9202–9211. [PubMed: 20869764]
68. Goldberger J, Berns EJ, Bitton R, et al. Electrostatic Control of Bioactivity. Angew Chem Int Ed. 2011; 50:6292–6295.

69. Cui H, Muraoka T, Cheetham AG, Stupp SI. Self-assembly of giant peptide nanobelts. Nano Lett. 2009; 9:945–951. [PubMed: 19193022]
70. Niece KL, Czeisler C, Sahni V, et al. Modification of gelation kinetics in bioactive peptide amphiphiles. Biomaterials. 2008; 29:4501–4509. [PubMed: 18774605]
71. Stendahl J, Rao M, Guler MO, Stupp SI. Intermolecular Forces in the Self-Assembly of Peptide Amphiphile Nanofibers. Adv Funct Mater. 2006; 16:499–508.
72. Zhang S, Greenfield MA, Mata A, et al. A self-assembly pathway to aligned monodomain gels. Nat Mater. 2010; 9:594–601. [PubMed: 20543836]
73. Capito RM, Azevedo HS, Velichko YS, et al. Self-assembly of large and small molecules into hierarchically ordered sacs and membranes. Science. 2008; 319:1812–1816. [PubMed: 18369143]
74. Chow LW, Bitton R, Webber MJ, et al. A bioactive self-assembled membrane to promote angiogenesis. Biomaterials. 2010; 32:1574–1582. [PubMed: 21093042]
75. Rożkiewicz DI, Myers BD, Stupp SI. Interfacial elf-Assembly of Cell-like Filamentous Microcapsules. Angew Chem Int Ed. 2011; 123:6488–6451.
76. Tysseling-Mattiace VM, Sahni V, Niece KL, et al. Self-assembling nanofibers inhibit glial scar formation and promote axon elongation after spinal cord injury. J Neurosci. 2008; 28:3814–3823. [PubMed: 18385339]
77. Shah RN, Shah NA, Lim MMDR, et al. Supramolecular design of self-assembling nanofibers for cartilage regeneration. Proc Natl Acad Sci US A. 2010; 107:3293–3298.
78. Mata A, Geng Y, Henrikson KJ, et al. Bone regeneration mediated by biomimetic mineralization of a nanofiber matrix. Biomaterials. 2010; 31:6004–6012. [PubMed: 20472286]
79. Sargeant TD, Guler MO, Oppenheimer SM, et al. Hybrid bone implants: self-assembly of peptide amphiphile nanofibers within porous titanium. Biomaterials. 2008; 29:161–171. [PubMed: 17936353]
80. Webber MJ, Han X, Prasanna-Murthy SN, et al. Capturing the stem cell paracrine effect using heparin-presenting nanofibres to treat cardiovascular diseases. J Tissue Eng Regen Med. 2010; 4:600–610. [PubMed: 20222010]
81. Rajangam K, Behanna H, Hui MJ, et al. Heparin binding nanostructures to promote growth of blood vessels. Nano Lett. 2006; 6:2086–2090. [PubMed: 16968030]
82. Angeloni NL, Bond CW, Tang Y, et al. Regeneration of the cavernous nerve by Sonic hedgehog using aligned peptide amphiphile nanofibers. Biomaterials. 2010; 32:1091–1101. [PubMed: 20971506]
83. Muraoka T, Koh C-Y, Cui H, Stupp SI. Light-triggered bioactivity in three dimensions. Angewandte Chemie (International ed in English). 2009; 48:5946–5949. [PubMed: 19582745]
84. Soukasene S, Toft DJ, Moyer TJ, et al. Antitumor activity of peptide amphiphile nanofiber-encapsulated camptothecin. ACS Nano. 2011; 5:9113–9121. [PubMed: 22044255]
85. Standley SM, Toft DJ, Cheng H, et al. Induction of Cancer Cell Death by Self-assembling Nanostructures Incorporating a Cytotoxic Peptide. Cancer research. 2010; 70:3026.
86. Bitton R, Schmidt J, Biesalski M, et al. Self-assembly of model DNA-binding peptide amphiphiles. Langmuir. 2005; 21:11888–11895. [PubMed: 16316129]
87. Cui H, Pashuck ET, Velichko YS, et al. Spontaneous and X-ray-triggered crystallization at long range in self-assembling filament networks. Science. 2010; 327:555–559. [PubMed: 20019248]
88. Ziserman L, Mor A, Harries D, Danino D. Curvature Instability in a Chiral Amphiphile Self-Assembly. Phys Rev Lett. 2011; 106:238105. [PubMed: 21770548]
89. Ziserman L, Lee HY, Raghavan SR, et al. Unraveling the Mechanism of Nanotube Formation by Chiral Self-Assembly of Amphiphiles. J Am Chem Soc. 2011
90. Shimada T, Lee S, Bates FS, et al. Wormlike Micelle Formation in Peptide-Lipid Conjugates Driven by Secondary Structure Transformation of the Headgroups. J Phys Chem B. 2009; 113:13711–13714. [PubMed: 19572667]
91. Shimada T, Megley K, Tirrell M, Hotta A. Fluid mechanical shear induces structural transitions in assembly of a peptide-lipid conjugate. Soft Matter. 2011; 7:8856–8861.
92. Webber MJ, Newcomb CJ, Bitton R, Stupp SI. Switching of self-assembly in a peptide nanostructure with a specific enzyme. Soft Matter. 2011; 7:9665–9671. [PubMed: 22408645]

93. Galler KM, Aulisa L, Regan KR, et al. Self-Assembling Multidomain Peptide Hydrogels: Designed Susceptibility to Enzymatic Cleavage Allows Enhanced Cell Migration and Spreading. J Am Chem Soc. 2010; 132:3217–3223. [PubMed: 20158218]
94. Galler K, Cavender A, Yuwono V, et al. Self-Assembling Peptide Amphiphile Nanofibers as a Scaffold for Dental Stem Cells. Tissue Eng Part A. 2008; 14:1–8. [PubMed: 18333800]
95. Marsden HR, Korobko AV, van Leeuwen ENM, et al. Noncovalent triblock copolymers based on a coiled-coil peptide motif. J Am Chem Soc. 2008; 130:9386–9393. [PubMed: 18582047]
96. Castelletto V, McKendrick JE, Hamley IW, et al. PEGylated amyloid peptide nanocontainer delivery and release system. Langmuir. 2010; 26:11624–11627. [PubMed: 20666427]
97. Rambaran RN, Serpell LC. Amyloid fibrils: abnormal protein assembly. Prion. 2008; 2:112–117. [PubMed: 19158505]
98. Vilar M, Chou H-T, Lührs T, et al. The fold of alpha-synuclein fibrils. Proc Natl Acad Sci USA. 2008; 105:8637–8642. [PubMed: 18550842]
99. Sachse C, Fändrich M, Grigorieff N. Paired beta-sheet structure of an Abeta(1-40) amyloid fibril revealed by electron microscopy. Proc Natl Acad Sci US A. 2008; 105:7462–7466.
100. Pagel K, Wagner S, Samedov K, et al. Random coils, beta-sheet ribbons, and alpha-helical fibers: One peptide adopting three different secondary structures at will. J Am Chem Soc. 2006; 128:2196–2197. [PubMed: 16478157]
101. Castelletto V, Hamley IW, Cenker C, Olsson U. Influence of Salt on the Self-Assembly of Two Model Amyloid Heptapeptides. J Phys Chem B. 2010; 114:8002–8008. [PubMed: 20496898]
102. Castelletto V, Hamley IW, Cenker Ç, et al. Influence of end-capping on the self-assembly of model amyloid peptide fragments. J Phys Chem B. 2011; 115:2107–2116. [PubMed: 21309578]
103. Han Y, He C, Cao M, et al. Facile disassembly of amyloid fibrils using gemini surfactant micelles. Langmuir. 2010; 26:1583–1587. [PubMed: 20000629]
104. Haryono A, Binder WH. Controlled arrangement of nanoparticle arrays in block-copolymer domains. Small. 2006; 2:600–611. [PubMed: 17193094]
105. Lin Y, ker AB, He J, et al. Self-directed self-assembly of nanoparticle/copolymer mixtures. Nature. 2005; 434:55–59. [PubMed: 15744296]
106. Sofos M, Goldberger J, Stone DA, et al. A synergistic assembly of nanoscale lamellar photoconductor hybrids. Nat Mater. 2009; 8:68–75. [PubMed: 19060890]
107. De Yoreo JJ, Wierzbicki A, Dove PM. New insights into mechanisms of biomolecular control on growth of inorganic crystals. Cryst Eng Comm. 2007; 9:1144–1152.
108. Grzelczak M, Pérez-Juste J, Mulvaney P, Liz-Marzán LM. Shape control in gold nanoparticle synthesis. Chem Soc Rev. 2008; 37:1783–1791. [PubMed: 18762828]
109. Yuwono VM, Burrows ND, Soltis JA, Penn RL. Oriented aggregation: formation and transformation of mesocrystal intermediates revealed. J Am Chem Soc. 2010; 132:2163–2165. [PubMed: 20112897]
110. Pouget EM, Bomans PHH, Goos JACM, et al. The initial stages of template-controlled CaCO3 formation revealed by cryo-TEM. Science. 2009; 323:1455–1458. [PubMed: 19286549]
111. Mahamid J, Sharir A, Gur D, et al. Bone Mineralization Proceeds through Intracellular Calcium Phosphate Loaded Vesicles: A Cryo-Electron Microscopy Study. J Struct Biol. 2011; 174:527–535. [PubMed: 21440636]
112. Yuan J, Müller A. One-dimensional organic–inorganic hybrid nanomaterials. Polymer. 2010; 51:4015–4036.
113. Maayan G, Popovitz-Biro R, Neumann R. Micelle directed synthesis of polyoxometalate nanoparticles and their improved catalytic activity for the aerobic oxidation of sulfides. J Am Chem Soc. 2006; 128:4968–4969. [PubMed: 16608327]
114. Wu S, Dzubiella J, Kaiser J, et al. Thermosensitive Au-PNIPA Yolk-Shell Nanoparticles with Tunable Selectivity for Catalysis. Angew Chem Int Ed. 2012; 51:2229–2233.
115. Tester CC, Brock RE, Wu C-H, et al. In vitro synthesis and stabilization of amorphous calcium carbonate (ACC) nanoparticles within liposomes. Cryst Eng Comm. 2011; 13:3975–3978.

116. Newcomb CJ, Bitton R, Velichko YS, et al. The Role of Nanoscale Architecture in Supramolecular Templating of Biomimetic Hydroxyapatite Mineralization. Small. 2012; 8:2195–2202. [PubMed: 22570174]

**117. Nudelman F, Pieterse K, George A, et al. The role of collagen in bone apatite formation in the presence of hydroxyapatite nucleation inhibitors. Nat Mater. 2010; 9:1004–1009. This manuscript describes a possible mechanism for mineralization of collagen *in vitro*, but more importantly it introduces the concept of direnctly visualizing dynamic protein-mineral interactions by cryogenic TEM. Monitoring mineralization and associating the mineral with domains of the collagen bundles in a hydrated state may lead to further understanding of biological processes that would otherwise be diffucult to observe *in vivo* using the techniques available to date. [PubMed: 20972429]

118. Fang P-A, Conway JF, Margolis HC, et al. Hierarchical self-assembly of amelogenin and the regulation of biomineralization at the nanoscale. Proc Natl Acad Sci US A. 2011; 108:14097–14102.

Research Highlight

- CryoTEM enables structural characterization of organic or organic-inorganic hybrid systems in a native, solvent-exposed state
- CryoTEM provides unique insight of dynamic nanoscale architectures in self-assembling, stimuli-responsive systems
- Recent advances in cryogenic techniques provides a means to characterize materials from nanometer to micron length scales

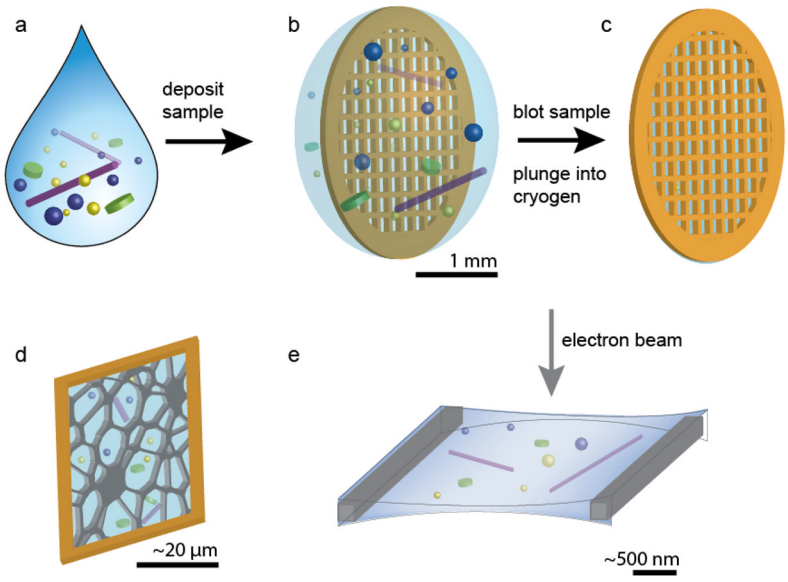

Figure 1.

Schematic of the sample preparation for cryo-TEM. (a) The solution containing self-assembled structures is (b) deposited on a TEM grid. (c) The grid is blotted with filter paper to remove excess solution and plunged into a cryogen. (d) The electron transparent film is supported by a carbon support and (e) imaged with the electron beam.

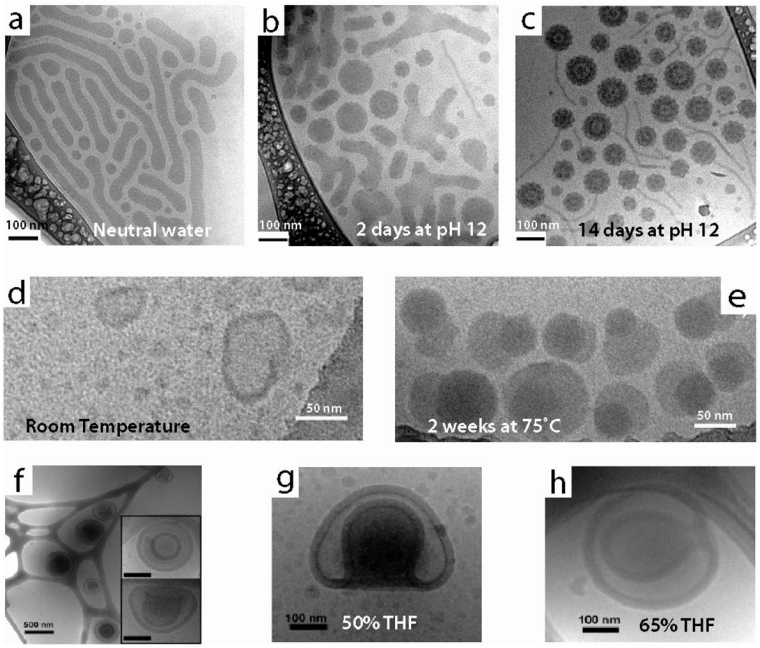

Figure 2.

Dynamics of stimuli-responsive block copolymer assemblies characterized by cryo-TEM. (a–c) Morphological evolution upon pH degradation of miktostar block copolymers. In neutral pH, (a) wormlike micelles are observed and at pH 12 (b–c) less ordered aggregates that were more spherical in shape evolved to raspberry vesicles with short chains. (d–e) Thermal annealing of hydrophilic-lipophilic-fluorophilic block copolymers. Spherical micelles and vesicles prepared at room temperature (d) phase segregate after thermal annealing into fluorophilic and lipophilic domains (e). (f–h) Solvent-dependent behavior of bowl-like polymerosome stomatocytes. Stomatocytes prepared by a dialysis method (f) show different sized openings depending on THF content (g–h). Panels (a–c) reprinted with permission from [28]. Copyright 2010 American Chemical Society. Panels (d–e) reprinted with permission from [35]. Copyright 2011 American Chemical Society. Panels (f–h) reprinted with permission from [41]. Copyright 2010 American Chemical Society.

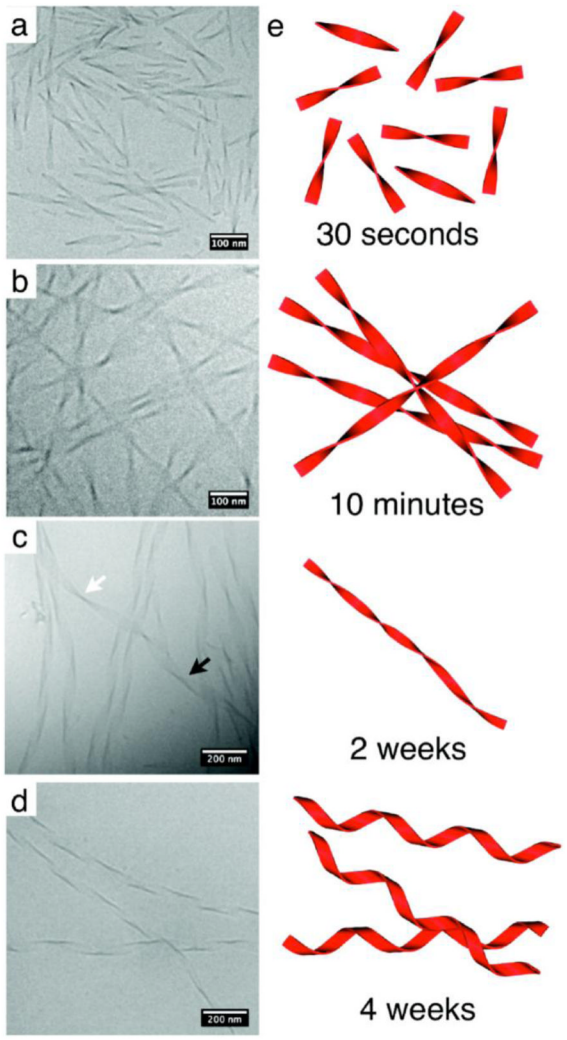

Figure 3.
Morphological transformation of phenylalanine-containing peptide amphiphiles from twisted ribbons to helical ribbons by cryo-TEM. (a) Short twisted nanostructures are observed 30 seconds following dissolution, (b) which grow in length by 10 minutes. (c) Following two weeks, the transformation from twisted ribbons (white arrow) to helical ribbons (black arrow) is observed. (d) Finally after 4 weeks of aging, only helical ribbons are present. Reprinted with permission from [9]. Copyright 2010 American Chemical Society.

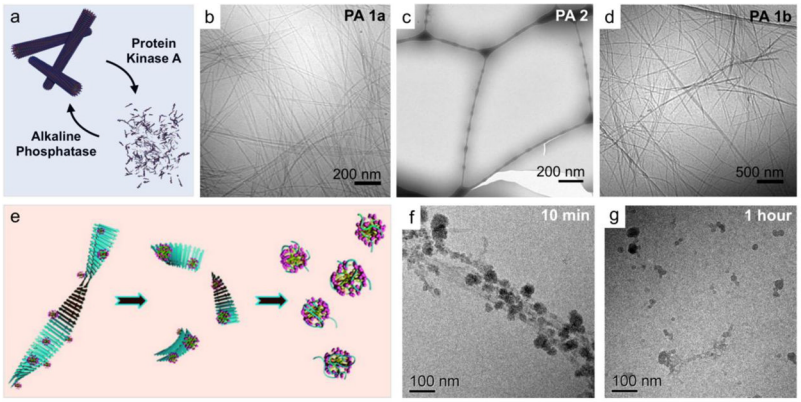

Figure 4.

Dynamic transformation of peptide-based supramolecular structures visualized by cryo-TEM. (a) An enzyme-responsive PA system designed with a substrate sequence was phosphorylated in the presence of PKA and unphosphorylated by ALP. (b) The high-aspect-ratio PA nanofibers (c) disassembled upon phosphorylation by PKA and (d) reformed as the phosphate group was cleaved by ALP. (e) To explore therapies for Alheimer's, cationic gemini surfactant micelles were explored for their ability disrupt the aggregation of amyloid fibrils *in vitro*. (f) The surfactant first adsorbs to the amyloid fibrils and (g) after an hour, the fibrils are broken into smaller nanoscopic aggregates. Panels (a–d) reprinted with permission from [92]. Copyright 2011 The Royal Society of Chemistry. Panels (e–g) reprinted with permission from [103]. Copyright 2010 American Chemical Society.

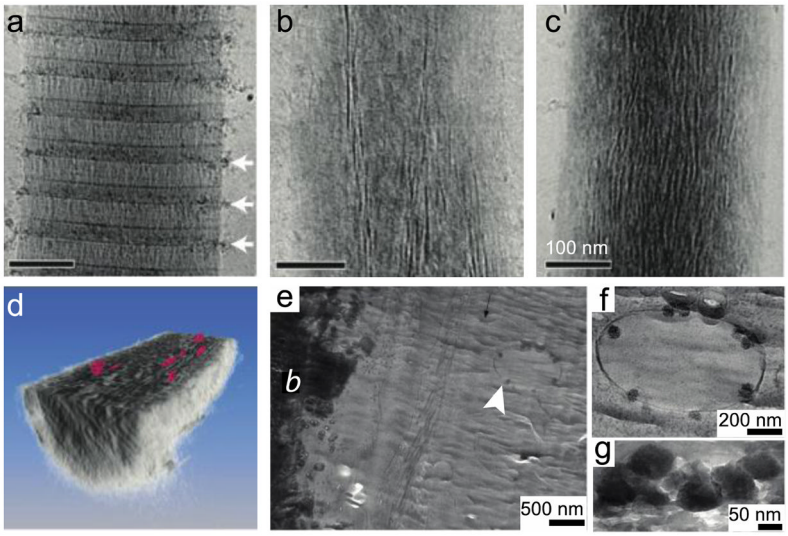

Figure 5.

Implementation of cryo-TEM to characterize transient biological organic-inorganic structures. To explore collagen mineralization, a model system with an amorphous mineral precursor was used. The collagen template was monitored over time by imaging the sample after (a) 24 hours, (b) 48 hours, and (c) 72 hours of mineralization. (d) A computer-generated three-dimensional representation from tomographic slices of a mineralized collagen bundle cut in cross section along the x–y plane to illustrate the plate-shaped apatite crystals (pink). To further investigate the role of amorphous calcium phosphate in developing mouse calvarial bone, (e) cryo-TEM of a vitrified section of tissue revealed the presence of intracellular amorphous calcium phosphate-containing vesicles (white arrowhead) in cells adjacent to the electron dense mineralized bone (labeled ***b)***. (f) A higher magnification of the vesicle in (e). (g) A freeze-dried cryo-section demonstrating the increased electron density from the mineral. Panels (a–d) reprinted with permission from [117]. Copyright 2010 Nature Publishing Group. Panels (e–g) reprinted with permission from [111]. Copyright 2011 Elsevier.